Int. J. Therm. Sci. (1999) 38, 142–147

Description of the temperature, humidity and concentration distribution in gas–liquid–solid fluidised beds

Stefan Heinrich, Lothar Mörl*

Institute of Process Equipment and Environmental Technology, Otto-von-Guericke-University, Magdeburg, Germany

(Received 7 January 1998, accepted 16 July 1998)

Abstract—This work presents physically based mathematical mass- and heat transfer models for processes of granulation, agglomeration and coating in fluidised beds. Starting from mass and energy balances, the models describe the influences of local liquid input, non-ideal solid and liquid mixing, heat transport by the solids, and a place-dependent degree of wetness. A coefficient for the heat or mass transfer solid–liquid film, solid–gas and gas–liquid films was defined. The place-dependent functions of gas and solid temperatures, gas humidity, gas enthalpy, liquid concentration, as well as the degree-of-wetness, are presented. The main conclusions of the model are the existence of an active zone in the liquid feed and, furthermore, of a central region in the fluidised bed, characterised by constant gas temperatures. © Elsevier, Paris.

heat and mass transfer / fluidised bed / spraying / evaporation / drying

Résumé — Étude de la distribution de la température, de l'humidité et de la concentration dans des lits fluidisés gaz–liquide–solide. Ce travail concerne la modélisation des transferts de masse et de chaleur pour l'analyse de la granulation, de l'agglomération et de la constitution de couches dans les lits fluidisés. Partant des bilans de masse et d'énergie, les modèles décrivent les influences de l'injection locale de liquide, du mélange non-idéal du solide et du liquide, du transfert thermique par les éléments solides et du degré d'humidité locale. Un coefficient de transfert de masse et un coefficient de transfert de chaleur solide–film liquide, solide–gaz et gaz–film liquide sont définis. On présente des fonctions donnant, localement, les températures du gaz et du solide, l'humidité du gaz, son enthalpie, la concentration en liquide et le degré d'humidité. Les conclusions principales du modèle concernent l'existence d'une zone active, correspondant à l'alimentation en liquide, et la région centrale du lit fluidisé, qui est caractérisée par des températures de gaz constantes. © Elsevier, Paris.

transfert de chaleur / transfert de masse / lit fluidisé / pulvérisation / évaporation / séchage

Nomenclature

A, A^*	particles surface, specific value	m^2, $m^2 \cdot m^{-3}$
c	specific heat capacity	$J \cdot kg^{-1} \cdot K^{-1}$
D	dispersion coefficient	$m^2 \cdot s^{-1}$
d	diameter	m
f_a	material surface factor	
H_{fB}	height of fluidised bed (expanded)	m
m	mass	kg
$\dot{m}_{FV}$	liquid mass flow per volume	$kg \cdot s^{-1}$
P	system pressure	Pa
R	general gas constant	$J \cdot kmol^{-1} \cdot K^{-1}$
r	specific liquid enthalpy of vaporisation	$J \cdot kg^{-1}$
T	temperature	K
w	velocity	$m \cdot s^{-1}$
X	water load of material	$kg \cdot W \cdot kg^{-1}_{\text{dry icy substance}}$
Y	water load of dry air	$kg \cdot W \cdot kg^{-1}_{\text{dry air}}$

Greek letters

α	heat-transfer coefficient	$W \cdot m^{-2} \cdot K^{-1}$
β, β^*	mass-transfer coefficient, modified value	$m \cdot s^{-1}$, $kg \cdot m^{-2} \cdot s^{-1} \cdot Pa^{-1}$
$\varepsilon, \varepsilon^*$	relative porosity, relative material volume	
ν	kinematic viscosity	$m^2 \cdot s^{-1}$

* Correspondence and reprints.

Subscripts, superscripts

A	air
App	apparatus
B	bed
DS	drying substance
E	entry
EP	expanded point
eff	effective
F	fluid (liquid phase)
G	adiabatic material steady-state point
N	nuclei
O	outlet
P	particle
S	solid
St	steam
Su	suspension
Sur	surface

1. INTRODUCTION

Solids in solutions, suspensions or melts are increasingly dried by spray granulation in fluidised beds. The liquid is sprayed into an upward-flowing gas stream, which causes the fluidisation of the solid bulk. Due to the enthalpy of the fluidising gas stream, the liquid evaporates and is then carried out with the gas stream. The solids dry snowball-like onto the particles' surface, or act as a binder for the agglomeration of the nuclei. A distinction between layering and agglomeration can be made. Assuming high heat and mass transfer rates, the process produces an adjustable, flowable, approximately spherical simultaneously dust-free granule. Furthermore, by recycling the gas partially or completely, the process becomes more energy efficient. The design of such plants is based on temperature- and concentration fields of the particle- and gas moisture because of the liquid input. In practice, an increased liquid feed may lead to sticking and clogging of the fluidised materials and a partial scaling of the apparatus. Hence, a decrease of the evaporated liquid mass and even a soaking of the entire bed may occur. Moreover, the liquid drips through the gas distribution plate. In this paper, physically based mathematical models under certain assumptions are described and compared with experimental results.

2. MATHEMATICAL DESCRIPTION

The operating range of the drying process is described by the overall mass balance of the injected and evaporated liquid. The exit condition can be read on the isenthalp in the Mollier diagram for wet air. This assumes adiabatic wetting of the heated fluidising air as well as a negligible enthalpy of the water. The intersection with the saturation line characterises the maximum amount of liquid the air can be loaded with and its temperature. By stating these numbers, the extent of the driving force is determined. A phenomenological description of the mass and energy balances of the components (air, liquid, and solid) has been worked out. As a result, the gradients of temperature and concentration can be determined. The basic distinguishing feature of the models is the degree of wetness $\varphi = A_{\text{wetted}}/A_{\text{total}}$. The latter characterises the wetted surface related to the total surface of the particle. The liquid is supposed to be deposited on the particles as a thin, film-like layer. It is also assumed that the liquid's temperature is the "adiabatic material steady-state temperature".

2.1. Constant degree of wetness

Assuming ideal mixing of the solids and plug-flow of the air, Mörl [1] suggested a model postulating ideal distribution of the liquid over all particles. As a result a height-dependent exponential curve for the moisture of the fluidising air $Y_A(z)$ with a inversely proportional air temperature $T_A(z)$ was determined:

$$Y_A(z) = Y_G - (Y_G - Y_{AE}) \exp[-A\,z] \tag{1}$$

$$T_A(z) = (h_{AE} - Y_A(z)r)/(c_{pA} + Y_A(z)\,c_{pSt}) \tag{2}$$

The balance around the dryer leads to the degree of wetness φ. Furthermore, a mean air temperature T_{Am} can be stated as well as a mean particle temperature T_{Pm}.

$$\varphi = -\frac{\dot{m}_A^* R_A}{\beta^* A^* P H_{fB} R_{St}} \cdot \ln\left[1 - \frac{\dot{m}_{DS,Su}/\dot{m}_A(X_S - X_O) + \dot{m}_{DS,N}/\dot{m}_A(X_{NE} - X_O)}{(Y_G - Y_{AE})}\right] \tag{3}$$

$$T_{Am} = \frac{1}{H_{fB} A}\left(\frac{r}{c_{pSt}} + \frac{B}{C}\right) \cdot \ln\left\{\frac{[c_{pSt}\exp(-AH_{fB}) - C]}{(c_{pSt} - C)}\right\} + \frac{B}{C} \tag{4}$$

$$T_{Pm} = T_G\varphi + T_{Am}(1 - \varphi) \tag{5}$$

with

$$A = (\beta^* \varphi\, A^* R_{St} P)/(\dot{m}_A^* R_A) \tag{6}$$

$$B = T_{AE}(c_{pA} + Y_{AE} c_{pSt})/(Y_G - Y_{AE}) - r \tag{7}$$

$$C = (c_{pA} + Y_{AE} c_{pSt})/(Y_G - Y_{AE}) + c_{pSt} \tag{8}$$

2.2. Height-dependent degree of wetness

With the introduction of the axial solids dispersion coefficient D_{ax}, Trojosky [2] completes the first model.

Only the liquid feed from above the fluidised bed is considered. Every single particle layer n is wetted by a certain amount of liquid corresponding to the surface coverage $(1-\varepsilon_{Sur})$. with $\varepsilon_{Sur} = 0{,}5\,(3\varepsilon-1)$. The sprinkled section of the particle's cross-section area is described by the degree of sprinkling $\phi(z) = \varepsilon_{Sur}^{n-}$, while the height-dependent degree of wetness $\varphi(z)$ is given by:

$$\varphi(z) = \varphi_{max}\, e^{\frac{z-H_{fB}}{B}} \tag{9}$$

The moisture and temperature of the air, the temperature of the particles and the liquid concentration are given by the following differential equations:

$$\frac{dY_A(z)}{dz} = \frac{\beta A^*}{\dot{V}_A^*}\varphi(z)(Y_G(z) - Y_A(z)) \tag{10}$$

$$\frac{dT_A(z)}{dz} = -\frac{\alpha_{AP}A^*}{c_{pA}\dot{m}_A}\left[\left(1-\varphi(z)\right)\left(T_A(z) - T_P(z)\right)\right] - \frac{r}{c_{pA}}\frac{dY_A(z)}{dz} \tag{11}$$

$$\frac{d^2T_P(z)}{dz^2} = -\frac{A^*}{D_{ax}c_{pP}\rho_P(1-\varepsilon)\dot{m}_A} \cdot\left[\alpha_{AP}(1-\varphi(z))\,(T_A(z) - \alpha_{PF}\varphi(z)(T_P(z) - T_G(z))\right] - T_P(z)) \tag{12}$$

$$\frac{d^2\rho_F(z)}{dz^2} = \frac{\dot{m}^*_{nozzle}\ln\varepsilon_{Sur}}{d_P D_{ax}}\varepsilon_{Sur}^{\frac{H_{fb}-z}{d_P}} + \frac{\dot{m}_A^*}{D_{ax}}\frac{dY_A(z)}{dz} \tag{13}$$

Once the liquid concentration $\rho_F(z)$ is known, the moisture $X(z)$ and the mean moisture of the solids $X(z)$ can be calculated as well as the liquid content of the fluidised bed m_F.

$$X(z) = \rho_F(z)A_{App}H_{fB}/m_P$$

$$m_F = \overline{X}(z)\,m_P = A_{App}\int_{z=0}^{z=H_{fB}}\rho_F(z)\,dz \tag{14,15}$$

Additionally, by using the degree of wetness $\varphi(z)$, the mean thickness of the liquid film $C(z)$ can be computed:

$$\overline{C}(z) = \frac{\rho_F(z)}{\varphi(z)}\frac{d_P}{6\,(1-\varepsilon)\,\rho_F} \tag{16}$$

2.3. Three-dimensional degree of wetness

Following Reppmann's discussion of the continuum, a system of differential equations was set up [3]. The degree of wetness φ varies along all Cartesian or cylindrical co-ordinates. To simplify the comparison of the models, it is restricted to the z-co-ordinate. The homogeneous fluidisation of the particles can be corrected by the axial and radial dispersion coefficients. At unsteady heat conduction within the granule the heat transfer interactions air–particle, air–liquid film and particle–liquid film can be described:

$$\frac{dY_A}{dz} = -\frac{\beta A^*\varepsilon^* f_a\varphi}{\dot{m}_A^*}(Y_A - Y_G) \tag{17}$$

$$\frac{dT_A}{dz} = -\frac{A^*\varepsilon^* f_a\,\alpha_{AP}}{\dot{m}_A^*(c_{pA} + Y_A c_{pSt})}\left\{(1-\varphi)\,(T_A - T_P) + \varphi\,(T_A - T_G)\left[1 + c_{pSt}(Y_G - Y_A)\frac{\beta}{\alpha_{AP}}\right]\right\} \tag{18}$$

$$\frac{d\rho_F}{dt} = D\,\nabla^2\rho_F + \beta\,A^*\varepsilon^* f_a\varphi\,(Y_A - Y_G) + \dot{m}_{FV} \tag{19}$$

$$\frac{d\rho_S}{dt} = D\,\nabla^2\rho_S = D\,\nabla^2\rho_P\varepsilon^* \tag{20}$$

$$c_{pF}\frac{d(\rho_F T_G)}{dt} = c_{pF}D\,\nabla^2(\rho_F T_G) + \alpha_{AP}A^*\varepsilon^* f_a\varphi\,(T_A - T_G) + \alpha_{PF}A^*\varepsilon^* f_a\varphi\,(T_P - T_G) + \beta A^*\varepsilon^* f_a\varphi\,(r + c_{pF}T_G)\,(Y_A - Y_G) + \dot{m}_{FV}r \tag{21}$$

$$c_{pS}\frac{d(\rho_S T_P)}{dt} = c_{pS}D\,\nabla^2(\rho_S T_P) + \alpha_{AP}A^*\varepsilon^*(1-\varphi)\,(T_A - T_G) - \alpha_{PF}A^*\varepsilon^*\varphi\,(T_P - T_G) \tag{22}$$

3. EXPERIMENTAL SET-UP

The experimental investigations were run with ambient air on a fluidised bed granulation plant of the institute with a diameter of 400 mm in the bed region (*figure 1*). By means of a special probe, temperature measurements throughout the bed could be made. The temperature distribution is influenced by the spraying technique, the liquid mass flow rate, air inlet temperature, and air mass flow rate, as well as by the nature and quantity of bed material.

The probe tube with a diameter of 12 mm is centrally inserted from the top into the apparatus. A 200 mm long tube with a diameter of 10 mm is attached at right-angles to the lower end. Along this tube, 5 small tubes with a diameter of 8 mm are arranged with a spacing of 50 mm. The PTFE-covered thermocouple is placed in these small tubes. The PTFE coverage serves as an insulation from heat conduction. A pump sucks an air stream through the tube along the thermoelements. To prevent the wetting of the thermocouple or collisions with particles the tube's opening is covered by a wire gauze. The bed region of the apparatus is insulated to ensure approximately adiabatic conditions. By rotating the probe, all bed heights and angles can be reached. The height was adjusted in increments of 5 mm up to a height of 50 mm in the distributor region, and in increments of 25 mm up to the nozzle-height of 380 mm. The angular adjustment was made in steps of 30°. Therefore, 24 levels with 60 positions each were read by means of an electronic data acquisition device.

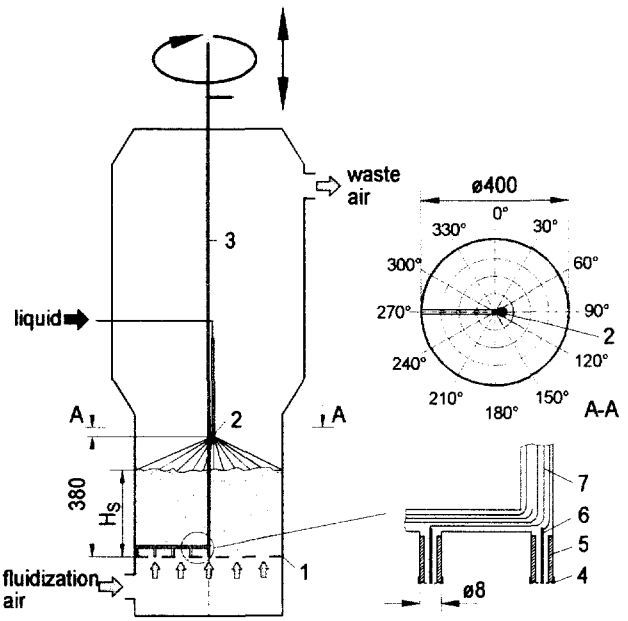

Figure 1. Probe for measuring air temperatures in the fluidised bed. 1. Air distribution plate. 2. Single fluid nozzle. 3. Probe tube. 4. Wire gauze. 5. PTFE-tube. Ni-CrNi thermocouple. 7. Compensation cable.

The experimental strategy was to increase the inlet air temperature and the mass flow rate of the liquid (water) with respect to a defined base experiment until saturation was reached. The water was injected by means of a hollow cone nozzle from a height of 300 or 380 mm vertically onto a bed of glass spheres ($d_P = 1.16$ and 3.05 mm) and a bed of wooden spheres ($d_P = 10$ mm), respectively. In order to investigate the influence of the height of the fluidised bed and air velocity on the heat- and mass transfer, the bulk porosity ($\varepsilon = 0.489$ and 0.718) and the Reynolds-number of the fluidising air ($Re = w_L\, d_P/\nu_L = 175$ and 520) were set to constant values corresponding to the respective solids.

The influence of the gas distribution plate on gas- and particle convection in the bed was validated using two kinds of heat-conducting plates. These plates with an aperture ratio of 17 % and an operating pressure loss of about 1 000 Pa were made of wood and copper.

4. RESULTS

Figure 2 shows the 3-dimensional air temperature readings of a fluidised bed of glass spheres with a bed height of 205 mm and following parameters: d_P = 1.16 mm; $m_P = 20$ kg; $\rho_P = 2\,471$ kg·m^{-3}; $T_{AE} = 120$ °C;

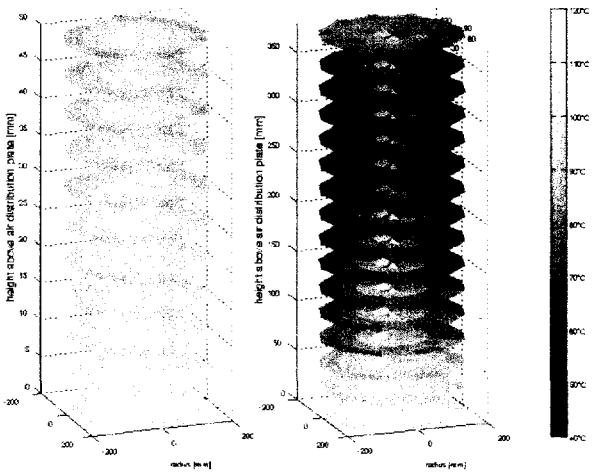

Figure 2. Measured air temperatures at $\dot{m}_F = 14$ kg·h^{-1} in a bed of glass spheres with $d_P = 1{,}16$ mm (left: air distribution plate area; right: general view).

specific air mass flow rate = 3.125 kg·s^{-1}·m^{-2}; water mass flow rate = 14 kg·h^{-1}; $Re = 175$. The nozzle was positioned in a height of 380 mm above the wooden gas distribution plate.

The radial and axial temperature gradients as shown in *figure 2* demonstrate the hollow-cone-like contour of the jet at non-ideal air- and solids distribution.

The average observed temperatures as a function of the probe location in the bed up to the calculated bed height were compared with the model calculations (using $Y_{AE} = 10$ g·kg^{-1}; $\dot{m}_{F,max} = 47.5$ kg·h^{-1}), as shown in *figure 3*. The data in *figure 3* were recorded at an increased water nozzle throughput of 24 kg·h^{-1}. Directly above the plate, the air temperature drops due to

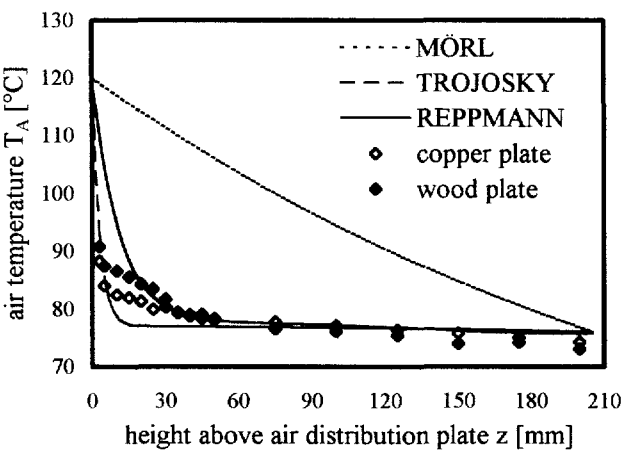

Figure 3. Measured air temperatures in comparison with the models at $\dot{m}_F = 24$ kg·h^{-1} in a bed of glass spheres with $d_P = 1{,}16$ mm.

particle convection and heat transfer between the hot air and the cooler particles. The air temperature reaches a nearly constant value over a considerable range. In the nozzle jet region, the air temperature drops according to the overall balance down to the outlet value because of the contact with the liquid on the particles and its evaporation. While running the experiments, it was noticed that the material of the plate does not affect the air temperature. By comparing the models in *figure 3*, it was found that the more exact results occur when the mixing is taken into consideration. Hence, ideal wetting, assumed in the model of Mörl, does not result in a fast air temperature drop down to a mean value in the experiment with the mono-dispersed glass spheres (specific particle surface $A^* = 6\,(1-\varepsilon)/d_P = 1\,622\ m^{-2}{\cdot}m^{-3}$ at $\varepsilon = 0.685$).

An interesting aspect is the verification with wooden spheres, since the specific surface is smaller ($A^* = 306\ m^2{\cdot}m^{-3}$ for $\varepsilon = 0.489$) and with it the mass transfer area for the evaporation. *Figure 4* shows the measured air temperatures compared with the Mörl model at water nozzle throughputs of 22.1 $kg{\cdot}h^{-1}$ and 55.6 $kg{\cdot}h^{-1}$. At a vertical liquid input from 380 mm ($\dot{m}_F = 22.1\ kg{\cdot}h^{-1}$, $\dot{m}_{AE} = 2.387\ kg{\cdot}s^{-1}{\cdot}m^2$; $Y_{AE} = 4\ g{\cdot}kg^{-1}$; $\dot{m}^*_{F,max} = 59.4\ kg{\cdot}h^{-1}$), the air temperatures approach each other, in contrast to *figure 3*. At a mass flow rate of 55.6 $kg{\cdot}h^{-1}$ the significant difference disappears nearly completely.

For the same parameters an attempt was made to analyse with regard to its moisture the air stream sucked through the probe tube (*figure 5*). The liquid content of the fluidising air is inversely proportional to the temperature, despite fluctuations eventually caused by a partial sucking of liquid mist into the upper bed regions. This supports the statement of constant wetting at low specific particle surface and high liquid inputs.

At high specific particle surface, the moisture of the fluidising gas diverges from the assumption of a

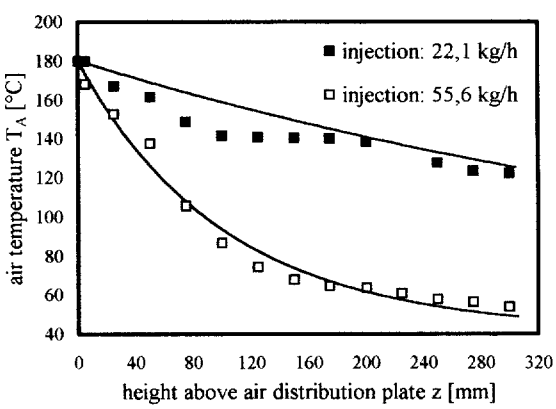

Figure 4. Measured air temperatures in comparison with the Mörl model in a bed of wooden spheres with $d_P = 10$ mm.

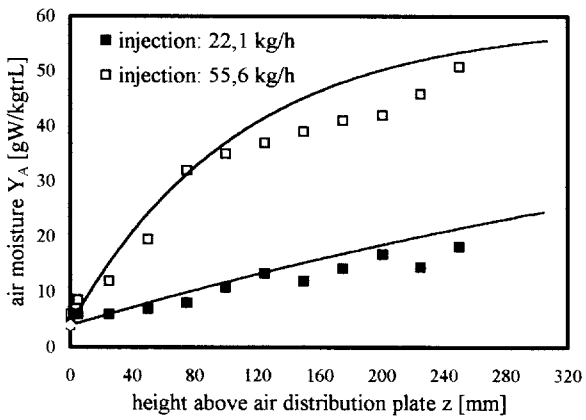

Figure 5. Measured air moistures in comparison with the Mörl model in a bed of wooden spheres with $d_P = 10$ mm.

constant degree of wetting. The feed liquid already evaporates in the upper bed regions. This is due to the opposite direction of the enthalpy effect and leads to a characteristic decreasing of the moisture profile.

5. CONCLUSIONS

With the models introduced, computation of the drying kinetics in fluidised bed spraying granulation plants becomes possible. The results of experiments on a gas–solid fluidised bed with top-down water spraying correspond well with the models in respect to the air temperature and moisture. The inhomogeneous air and solid distribution was established on the basis of the gradients occurring. After a dry heat transfer above the plate, one gets heated particles in upper regions, where heat disposal through vaporisation and the formation of a constant mean bed temperature T_B can be observed, pointing up too the advantage of the heat and mass transfer in fluidised beds. In the sprayed upper bed regions the mass transfer zone can be characterised as wet, from which cool particles go to plate regions and take up heat.

The dispersion of the 3 phases has therefore an essential influence. The axial direction is placed in an order of magnitude over the radial direction. A considerable number of differential equations must be solved, which depend on experimental conditions and the fluidised bed apparatus employed. The calculations according to Trojosky and Reppmann were carried out with an axial dispersion coefficient D_{ax} by Kawase and Moo Young [4]:

$$D_{ax} = \frac{w_{surplus}\, D_{App}}{1.72 \left(\dfrac{w^2_{surplus}}{9.81\, D_{App}} \right)^{1/3}} \quad \text{with } w_{surplus} = w_{eff} - w_{EP} \tag{23}$$

The term in the denominator of equation (23) describes a Péclet number. For the glass spheres, $\dot{m}^*_{AE} = 3.125\ kg \cdot s^{-1} \cdot m^{-2}$ and $D_{ax} = 0.51\ m^2 \cdot s^{-1}$; for the wooden spheres, $\dot{m}^*_{AE} = 2.387\ kg \cdot s^{-1} \cdot m^{-2}$ and $D_{ax} = 0.37\ m^2 \cdot s^{-1}$. Consequently, low fluidisation velocity causes a smaller dispersion of the locally fed liquid. However, the drop down of the mass transfer area meets the requirement of wetted particles.

The height in which the region with constant bed temperature T_B begins-and with this the drying rate—does not depend on the quantity of the injected liquid. but rather on the solids used and their diameter. By increasing the throughput of the liquid and reducing the bed heights and with enlarged particle diameters (small NTU—number of transfer units). T_B becomes less detectable. Then, the lower and upper regions begin to overlap, which can lead to a higher particle agglomeration. Optimisation of the necessary bed height is possible with the models studied when there is low risk of agglomerate formation at granulation and coating processes.

An interesting aspect, especially for thermolabile materials. is that the entire temperature level in fluidised beds is lowered by submerged nozzles and that a punctual liquid feed leads to the desired agglomeration. whereas a fine liquid distribution causes the opposite effect.

If the local degree of wetness were known, it would be worthwhile for further modelling to investigate the installation of heating surfaces as sources of heat into dry zones. Accordingly, the shape and the locus-dependent intensity of the jet should be described using improved physically based mathematical equations. In addition, measurements of the air moisture should be done to back up the equations. Furthermore, the influences of impeller agitators and controlled fluid flow [5] need to be tested. The objective is the application to dynamic batch processes.

REFERENCES

[1] Mörl L., Wirbelschichtgranulationstrocknungsanlagen, Thesis, B TH Magdeburg, 1981.

[2] Trojosky M., Modellierung des Wärme- and Stofftransportes in flüssigkeitsbedüsten Gas/Feststoff-Wirbelschichten, Thesis, TU Magdeburg, 1991.

[3] Reppmann D., Experimentelle and theoretische Untersuchungen zur Eindüsung von Flüssigkeiten in eine Wirbelschicht, Thesis, TU Magdeburg, 1990.

[4] Kawase Y., Moo-Young M., Gas-bubble hold-up and axial dispersion coefficient of emulsion phases in fluidised beds, Can. J. Chem. Eng. 65 (3) (1987) 505–507.

[5] DDR-Patent Nr. 119304, 23/04/1975.